IEEE Access
Multidisciplinary | Rapid Review | Open Access Journal

Received February 10, 2020, accepted February 24, 2020, date of publication February 27, 2020, date of current version March 10, 2020.

Digital Object Identifier 10.1109/ACCESS.2020.2976785

Study of Magnetic Noise of a Multi-Annular Ferrite Shield

JIXI LU[1,3], DANYUE MA[1], KE YANG[1], WEI QUAN[1], JUNPENG ZHAO[1], BOZHENG XING[1], BANGCHENG HAN[1,2,3], AND MING DING[1,3]

[1]Research Institute for Frontier Science, Beihang University, Beijing 100191, China
[2]School of Instrumentation and Optoelectronic Engineering, Beihang University, Beijing 100191, China
[3]Quantum Sensing Center, Zhejiang Lab, Hangzhou 310000, China

Corresponding author: Ming Ding (mingding@buaa.edu.cn)

This work was supported in part by the National Natural Science Foundation of China under Grant 61903013, Grant 61773043, and Grant 61703025, and in part by the Major Scientific Research Project of Zhejiang Lab under Grant 2019MB0AE01.

ABSTRACT Ferrites are promising nonmetallic materials used for the fabrication of low-noise magnetic shields because they possess high permeability and high electrical resistivity. However, large-sized ferrite components are difficult to fabricate or machine. In this study, we develop a cylindrical ferrite shield that consists of five annuli and two lids with an inner volume of ϕ11.2 cm $\times$ 22.5 cm. Although this structure contains gaps between different components, it eases considerably the fabrication and machining process as compared to the entire module. The magnetic noise is measured by a spin-exchange relaxation-free atomic magnetometer, and the detrimental effects of the gaps are analyzed quantificationally using the finite element method. Our research results indicate that compared with the ferrite shield without gaps, the magnetization noise increases by 34.1%. Nonetheless, the magnetic noise at the center of the ferrite shield achieves $5.5f^{-1/2}$ fT, which is much lower than that of μ-metal shields with a similar size. If the gap width can be reduced to be smaller than 0.01 mm, the increase of the magnetization noise will be less than 4.9%, which can be negligible in practical applications. Our study provides a low-cost, readily available, and low-noise ferrite shield structure.

INDEX TERMS Ferrite, magnetic shield, magnetic noise, atomic magnetometer.

I. INTRODUCTION

Modern atomic sensors, such as atomic magnetometers, atomic gyroscopes, and atomic clocks, are highly sensitive to magnetic fields [1]–[3]. High-performance magnetic shields, which attenuate external magnetic fields, are indispensable for a stable magnetic environment [4]–[8]. Typically, magnetic shields are multilayered nested shells made of a high-permeability metal such as μ-metal ($\mu\sim10^4\mu_0$, where μ_0 is the vacuum permeability) with shielding factors even better than 10^6. However, the innermost layer of μ-metal shields generates magnetic noise in the range of 1–10 fT Hz$^{-1/2}$ at the center of the shield attributed to Johnson noise (its electrical resistivity $\rho\sim10^{-6}$ Ωm) [9]–[12]. This level of magnetic noise limits the performance of high-precision atomic sensors [13].

In recent years, ferrites have been studied as ideal materials for magnetic shields owing to their high permeability ($\mu\sim10^2\mu_0-10^4\mu_0$) and much higher electrical resistivity ($\rho\sim0.1\Omega$m $-$ $10^6\Omega$m) [14], [15]. Therefore, a ferrite enclosure can be used as the innermost shield to suppress the magnetic noise generated by μ-metal shields. Ferrite shields were first investigated by Kornack *et al*. [10]. They developed a ferrite shield with an inner volume of ϕ10 cm $\times$ 10 cm and a thickness of 1 cm. The sidewall of the shield was machined from an entire ferrite block [14]. The observed noise was 25 times lower as compared to that for a similar-sized μ-metal shield, and most of the magnetic noise was attributed to magnetization noise. Consequently, ferrite shields have been used in many atomic sensors, such as atomic magnetometers, co-magnetometers, and nuclear magnetic resonance gyroscopes [16]–[20].

Compared to high-permeability metals, ferrites are difficult to fabricate and machine, especially if large dimensions are needed. To this end, we devised a cylindrical, multi-annular ferrite shield and studied its magnetic noise characteristic. The purpose of this study is to provide a low-cost, readily available, and low-noise ferrite shield. Because

The associate editor coordinating the review of this manuscript and approving it for publication was Jenny Mahoney.

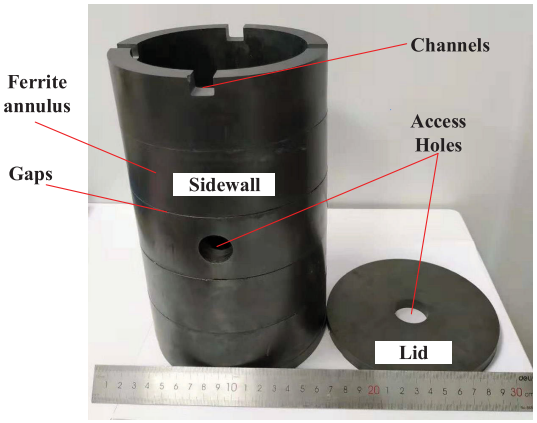

FIGURE 1. The ferrite shield consisting of five annuli and two lids.

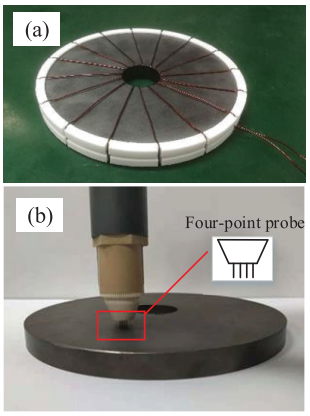

FIGURE 2. (a) A toroidal coil with 16 turns wound over the lid. The white component is a Teflon part to fasten the coils. (b) Four-point probe on the ferrite lid with a tip spacing of 1 mm. The measurement was conducted at 22.9 ± 0.5 °C.

short but large-diameter ferrite annuli are easy to fabricate and there are some commercial products with specific dimensions [21], the referred structure is much easier to develop compared to the entire module (like the ferrite shield developed by Kornack *et al*), albeit at the cost of gaps between different components. First, we measured the complex permeability, the electrical resistivity, and the shielding factor of the ferrite. The former two parameters were used to analyze the magnetic noise of the ferrite itself, and the latter was measured to validate the efficacy against the magnetic noise from the μ-metal shield. Subsequently, we measured the magnetic noise of the ferrite shield by a spin-exchange relaxation-free (SERF) atomic magnetometer, and analyzed quantificationally the effect of gaps on the magnetic noise with the use of the finite element method (FEM). Our study indicates that although gaps increase magnetic noise, this ferrite shield can still exhibit a low-noise magnetic environment analogous to that without gaps.

II. EXPERIMENTAL SETUP AND METHOD

A. FERRITE SHIELD

Our ferrite shield is a custom-made assembly which consists of a sidewall and two end lids (Fig. 1). There are mainly two classes of soft magnetic ferrite materials: MnZn and NiZn ferrites. The former have higher permeability, and thus they are more suitable for magnetic shields. The ferrite material we used was MnZn ferrite ($Zn_{0.45}Mn_{0.49}Fe_{2.04}O_4$) with a nominal relative permeability of 10^4 ($\pm 10\%$) at 25 °C. The total and inner volumes were $\phi 14$ cm × 24.5 cm and $\phi 11.2$ cm × 22.5 cm, respectively. The sidewall consisted of five ferrite annuli. Each of these had a height of 45 mm, an outer diameter of 140 mm, and a wall thickness of 14 mm. The diameter and thickness of each lid were 140 mm and 10 mm, respectively. The annuli were glued together, and gap widths in the range of 0.01–0.1 mm were created between them owing to the glue and the uneven mating surfaces. There were four access holes (2.2 cm in diameter) along the radial axis in the sidewall, and two access holes (2.8 cm in diameter) along the longitudinal axis in the lids. There were four small channels on the top of the sidewall that provided access to electrical wires and water-cooled tubes.

B. PERMEABILITY, ELECTRICAL RESISTIVITY AND SHIELDING FACTOR

The complex permeability and the electrical resistivity are two of the most important parameters determining the magnetic noise of the ferrite shield. Therefore, we first measured these two parameters. The complex permeability ($\mu = \mu' - i\mu''$) was measured using the impedance measurement method [10], [22]–[24]. This method has been demonstrated in the research on the ferrite shield in [10] and [24]. A toroidal coil with 16 turns was wound over the lid (shown in Fig. 2(a)). We used an LCR meter (E4980A, Keysight) to measure the coil's impedance at 20 Hz, and calculated the complex permeability using

$$\mu' = \frac{l_e}{A_e {N_{\text{coil}}}^2} L, \tag{1}$$

$$\mu'' = \frac{l_e}{2\pi A_e {N_{\text{coil}}}^2 f} (R - R_w), \tag{2}$$

where L and R are the measured inductance and resistance respectively, R_w is the resistance of the wire, A_e is the sectional area, N_{coil} is the number of turns, f is the frequency and l_e is the equivalent length

$$l_e = \frac{\pi (d_o - d_i)}{\ln (d_o / d_i)}, \tag{3}$$

where d_o and d_i are the outer and inner diameters, respectively.

During the measurement process, the ferrite lid was placed in a single-layered μ-metal magnetic shield that was used to keep the magnetic field stable. The measurement was conducted with different driving fields in the range of $\mu_0 H_{\text{dr}} = 0.36 - 1.46\mu$T. The measurement error increased significantly at lower driving fields. Given that the ferrite was used as the innermost shield (where the magnetic field was

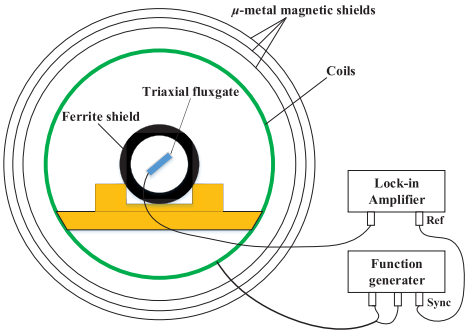

FIGURE 3. Schematic of the experimental setup used to measure the shielding factor of the ferrite shield. Ref: Reference input. Sync: Synchronization.

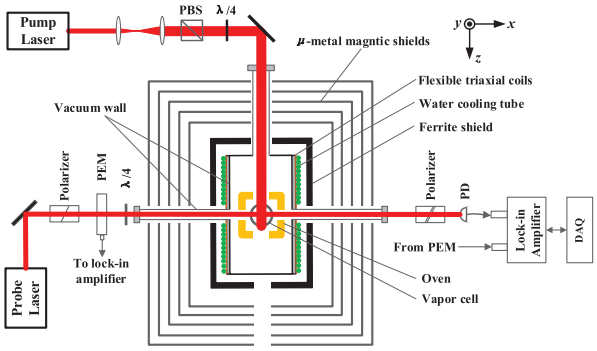

FIGURE 4. Schematic of the SERF atomic magnetometer for measuring the magnetic noise. The longitudinal direction of the ferrite was along the *z* axis.

nearly zero), the permeability used to analyze the shielding factor and the magnetic noise should be the initial permeability. In the cases of applied magnetic fields with small amplitudes, the magnetization curve was in the Rayleigh region [25]:

$$\mu = \mu_{\mathrm{i}} + \eta H, \tag{4}$$

where μ_{i} is the initial permeability, and η is the Rayleigh constant. Therefore, the measured complex permeability with different driving fields were extrapolated linearly to a zero driving field.

The four-point probe method was used to measure the electrical resistivity [26]. The four-point probe had a tip spacing (d) of 1 mm and touched the lid's surface (as shown in Fig. 2(b)). A digital multimeter (34401A, Agilent) was connected to it. The electrical resistivity was then determined using $\rho = R_{\mathrm{fp}} C_{\mathrm{cf}}$, where R_{fp} is the resistance measured by the multimeter, and C_{cf} is the correction factor determined by the geometry of the object. Herein, $C_{\mathrm{cf}} = 2\pi d$.

To validate the efficacy of the ferrite shield against the magnetic noise from the μ-metal shield layer, we measured its magnetic shielding factor. The magnetic shielding factor S can be defined as $S = B_{\mathrm{ex}}/B_{\mathrm{in}}$, where B_{ex} is the externally applied magnetic field, and B_{in} is the internally measured magnetic field. The schematic of the experimental setup for measuring the shielding factor is shown in Fig. 3. Three nested cylindrical μ-metal shields with an inner diameter of 40 cm were used to attenuate the ambient magnetic field. The thickness of each μ-metal layer was 1.5 mm. Coils were wrapped around a cylindrical frame with a 35 cm diameter, and were driven by a function generator (33500B, Keysight). Radial and longitudinal magnetic fields were generated by saddle coils and Lee-Whiting coils, respectively [27], [28]. The μ-metal shield can affect the coil constants owing to the coupling effect. Therefore, we calibrated the coil constants in the μ-metal shield before we measured the magnetic shielding factor. The ferrite shield was placed at the center of the coils, and a triaxial fluxgate (Mag-03, Bartington Instruments) was installed at the center of the ferrite shield. We applied AC magnetic fields at the frequency range of 1–150 Hz in the radial and longitudinal directions, and measured the fluxgate's response with a lock-in amplifier (SR830, Stanford Research Systems). Accordingly, both the radial and longitudinal shielding factors were obtained. The amplitude of the applied magnetic field may affect the permeability of magnetic shields, and could thus change the shielding factor. The ferrite was used as the innermost shield where the magnetic field was extremely small. Therefore, the amplitude of the applied magnetic field was set to be as small as 300 nT. In the presence of a magnetic field with this amplitude, the permeability was close to the initial permeability.

C. MAGNETIC NOISE

A SERF atomic magnetometer was set up to measure the magnetic noise (Fig. 4). Five nested cylindrical μ-metal magnetic shields with length-diameter ratio of 1.5 and inner diameter of 32 cm were used to attenuate the external magnetic field. The thickness of each μ-metal layer was 1.2 mm. A spherical glass vapor cell (25 mm in diameter), which contained a small droplet of potassium metal, was filled with nearly 1.2 atm ^{4}He as the buffer gas and 50 torr N_2 as the quenching gas. The vapor cell was heated to 200 °C using an electronic heater with an AC current at a frequency of 100 kHz. A vacuum enclosure with water cooling tubes was used for thermal insulation. A set of flexible coils were also glued to it to generate magnetic fields. A circularly polarized pump beam, near the center of the D1 line, polarized the potassium atoms along the z axis [29]. The spin precession caused by the magnetic field was detected by a linearly polarized probe beam tuned 0.2 nm away from the center of the D1 line. The probe beam was along the x axis. The polarization angle was measured using a photoelastic modulator (PEM-100, Hinds Instruments) and a lock-in amplifier (HF2LI, Zurich Instruments). Both beams were originated from independent distributed Bragg reflector (DBR) lasers. The diameters of the pump and probe beams were 20 mm and 3 mm, respectively. All three components of the magnetic field were zeroed by the coils, and the magnetometer was sensitive to the magnetic field along the y axis.

First, in the absence of the ferrite, the frequency response of the magnetometer was measured by applying an AC magnetic field (rms value of 10 pT) along the y axis at several frequencies. Next, we measured the probe noise spectrum and the total noise spectrum of the magnetometer in volts. The former was measured by turning off the pump light and magnetic field coils. These two noise spectra were converted to units of magnetic flux density (fT) by dividing them by the frequency response, and accordingly the probe noise and the sensitivity of the magnetometer were obtained. Subsequently, we installed the ferrite shield, degaussed the shield system and measured the residual magnetic field in the central region (4 cm $\times$ 4 cm $\times$ 4 cm). Finally, we repeated the first two procedures in the presence of the ferrite shield and obtained the magnetometer's sensitivity.

The fundamental sensitivity limits of SERF magnetometers attributed to spin projection noise are estimated to be on the order of aT $\mathrm{Hz}^{-1/2}$ $\mathrm{cm}^{-3/2}$ [13]. Therefore, the sensitivity is primarily limited by magnetic and probe noise. We optimized the signal to noise ratio of the magnetometer to make the probe noise significantly smaller compared with the sensitivity of the magnetometer. Consequently, according to the experiment stated in the above paragraph, we could obtain the magnetic noise of the μ-metal and ferrite shields.

After the measurement of the magnetic noise, we analyzed the magnetic noise of this multi-annular ferrite shield. Using the fluctuation-dissipation theorem [10], [11], the direct calculation of the magnetization noise at a point in the shield can be converted to a calculation of the power loss in the shield material generated by a hypothetical current-carrying excitation coil located at the same point. Based on this theorem, the magnetization noise can be calculated using

$$\delta B_{\mathrm{magn}} = \sqrt{\frac{4k_{\mathrm{B}}T\mu''}{2\pi f}}\frac{\sqrt{\int_V H^2 dV}}{A_{\mathrm{hc}}I}, \tag{5}$$

where H is the amplitude of the magnetic field intensity generated by a current I flowing in the coil, the integral is carried out over the volume V of the shield material, and A_{hc} is the area of the hypothetical coil. It is difficult to obtain an analytical expression if gaps are considered. Therefore, we calculated $\int_V H^2 dV$ numerically using FEM, and then used (5) to obtain δB_{magn}.

The schematic of the simulation model is shown in Fig. 5. A current-carrying (1 A, DC) loop with a diameter of 3 mm was placed at the center of the shield to produce an excitation magnetic field. All the parameters (except the gap width) of the ferrite shield model are same to the measured values. The gaps between different parts of the shield were also selected as 0 mm, 0.01 mm, 0.05 mm, and 0.10 mm.

FIGURE 5. Schematic of the magnetization noise simulation model (not to scale). A current-carrying (1 A, DC) loop with a diameter of 3 mm is placed at the center of shield to produce the excitation magnetic field. All the parameters (except the gap width) of the ferrite shield model are same to the measured values. The gaps between different parts of the shield are 0 mm, 0.01 mm, 0.05 mm, and 0.10 mm.

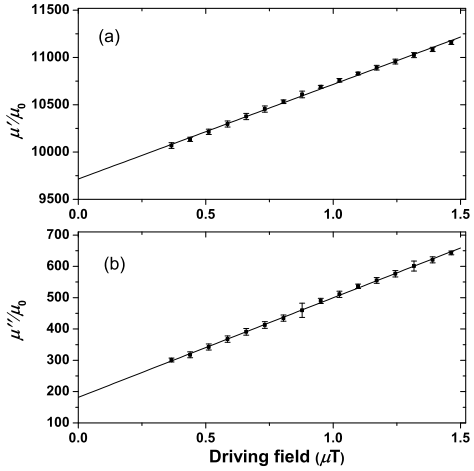

FIGURE 6. Real part (a) and imaginary part (b) of relative permeability as a function of the driving field.

III. RESULTS, ANALYSES AND DISCUSSION

A. PERMEABILITY, ELECTRICAL RESISTIVITY, AND SHIELDING FACTOR

Fig. 6 shows the real part and the imaginary part of the relative permeability as a function of the driving field. The extrapolated values to the zero driving field are $\mu'/\mu_0 = 9715 \pm 24$ and $\mu''/\mu_0 = 182 \pm 5$. The electrical resistivity was measured at 10 different locations in the central region of the lid, and the measured mean value was 0.127 ± 0.020 Ωm. The measured shielding factors were found to be generally constant over the frequency range 1–150 Hz as shown in Table 1. The average radial and longitudinal shielding factors are 509.2 ± 3.0 and 49.5 ± 0.2, respectively. Note that the shielding factor at 50 Hz was not measured owing to the power frequency interference.

Based on our previous study [30], the gaps have significant effects on the shielding factor. Therefore, we calculated the shielding factor numerically using the FEM with a commercial analysis software (Ansoft Maxwell) [30], [31]. All the parameters of the simulation model except the gap width of the ferrite shield were the same to those of the experimental setup, as described in Section II.B. The gap widths between different parts of the shield were selected as 0 mm, 0.01 mm, 0.05 mm, and 0.10 mm. Consequently, we obtained

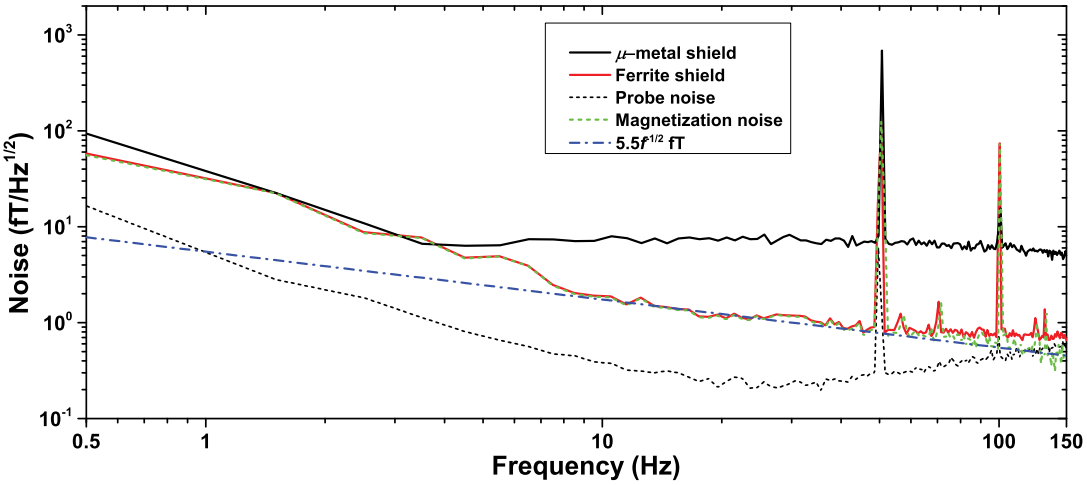

FIGURE 7. Noise spectra of the SERF magnetometer. The black line is the sensitivity of the SERF magnetometer in the absence of the ferrite shield. The red line is the sensitivity of the SERF magnetometer in the presence of the ferrite shield, which achieves 0.8–1.0 fT $Hz^{-1/2}$ at frequencies higher than 40 Hz. The black dashed line is the probe noise of the magnetometer in units of magnetic flux density (fT). The green dashed line is the magnetization noise. The blue dot-dashed line indicates $5.5f^{-1/2}$ fT. The peaks at 50 Hz and 100 Hz are attributed to the power frequency noise. The probe noise is considerably smaller than the sensitivity of the SERF magnetometer below 50 Hz. Therefore, the red line and the green dashed line overlap in this frequency range.

TABLE 1. Measured shielding factors at different frequencies.

Frequency (Hz)	Radial	Longitudinal
1	505.4 ± 19.6	49.2 ± 0.9
10	504.2 ± 1.5	49.2 ± 0.3
20	506.6 ± 2.6	49.4 ± 0.3
30	509.6 ± 1.5	49.4 ± 0.2
40	506.0 ± 2.0	49.4 ± 0.2
60	506.6 ± 1.8	49.6 ± 0.2
70	508.4 ± 2.1	49.6 ± 0.2
80	509.6 ± 2.8	49.6 ± 0.2
90	507.8 ± 2.4	49.7 ± 0.2
100	512.6 ± 2.8	49.8 ± 0.2
110	510.2 ± 2.2	49.6 ± 0.2
120	512.0 ± 2.1	49.4 ± 0.2
130	512.6 ± 1.7	49.5 ± 0.2
140	513.9 ± 1.8	49.6 ± 0.2
150	512.0 ± 2.0	49.8 ± 0.1

the simulated magnetic field at the central part of shield and the shielding factors. Table 2 shows the comparison of the measured and simulated shielding factors. The shielding factors decrease with increases of the gap width. Compared with the simulation results (using FEM with gap $\delta = 0$ mm), the measured radial and longitudinal shielding factors reduce by 32.5% and 89.1%, respectively, while the simulated radial and longitudinal shielding factors decrease by 7.2%–21.4% and 65.5%–94.1% with $\delta = 0.01$ mm–0.10 mm, respectively. Further, the simulations also indicate that the average gap width of the real ferrite shield is close to 0.05 mm and 0.10 mm.

B. MAGNETIC NOISE

Fig. 7 shows the magnetic field sensitivities for the SERF magnetometer in the presence and absence of the ferrite shield and the probe noise. After the installation of the ferrite shield, the residual magnetic fields in the central region along

TABLE 2. Comparison of the measured and simulated (using FEM) values of the shielding factors.

Method	Radial	Longitudinal
Measured	509.2	49.5
FEM (δ=0 mm)	754.3	455.8
FEM (δ=0.01 mm)	700.3	157.1
FEM (δ=0.05 mm)	661.5	50.0
FEM (δ=0.10 mm)	592.8	26.9

the x axis, the y axis and the z axis were 0.2 nT, 0.2 nT and 0.6 nT, respectively. The gradient along three axes were all smaller than 0.1 nT/cm. In Fig. 7, the probe noise (black dashed line) is significantly smaller than the magnetic field sensitivity. The magnetic field sensitivity in the absence of the ferrite shield is in the range of 5–7 fT $Hz^{-1/2}$ at frequencies above 3 Hz (black line). This is primarily attributed to the Johnson noise from the inner layer μ-metal shield. The sensitivity is in good agreement with the expected value of 6.9 fT $Hz^{-1/2}$ calculated using

$$\delta B_J = \frac{\mu_0}{D_i/2}\sqrt{\frac{k_B T t}{\rho}}\sqrt{\frac{2}{3\pi}G}, \tag{6}$$

where D_i is the inner diameter of the shield, k_B is Boltzmann's constant, T is the temperature in Kelvin, t is the thickness of the shield, and G is a factor related to the length-diameter ratio and is ≈ 4.6 [11]. For μ-metal, $\rho \approx 6.25 \times 10^{-7}\Omega$m.

Therefore, although the transverse shielding factor of the ferrite shield is lowered owing to the gaps, the Johnson noise from the inner layer μ-metal shield can still be attenuated to be on the order of 0.01 fT $Hz^{-1/2}$. The magnetic field sensitivity in the presence of the ferrite shield was primarily limited by two noise factors: the magnetic noise generated by the ferrite shield and the probe noise of the magnetometer.

TABLE 3. Comparison of the measured and simulated (using FEM) magnetization noise.

Methods	Magnetization noise ($f^{-1/2}$ fT)
Measured	5.5
FEM (δ= 0 mm)	4.1
FEM (δ= 0.01 mm)	4.3
FEM (δ= 0.05 mm)	5.0
FEM (δ= 0.10 mm)	5.3

The former includes Johnson and magnetization noise. Based on the measured electrical resistivity, the Johnson noise of our ferrite shield can be estimated to be 0.15 $\pm$ 0.01 fT Hz$^{-1/2}$ using (6), which is much smaller than the magnetization noise at lower frequencies. Therefore, we ignored the Johnson noise, and then extracted the magnetization noise from the magnetic sensitivity using $\delta B_{\text{magn}} = \sqrt{\delta B_{\text{f}}{}^2 - \delta N_{\text{pr}}{}^2}$ (green dashed line), where δB_{f} is the magnetic field sensitivity in the presence of the ferrite shield (red line), and δN_{pr} is the probe noise (black dashed line). From Fig. 7, we can see that the magnetization noise reveals a 1/f power spectrum at frequencies above 10 Hz. It is close to the blue dot-dashed line which indicates a noise of $5.5f^{-1/2}$ fT. The deviation below 10 Hz is attributed to the low-frequency vibration and other unexpected noise sources.

Table 3 shows a comparison of the measured and simulated (using FEM) values of magnetization noise. We can observe that the gaps have a detrimental effect on the magnetization noise. The magnetization noise increases with the increase of gap widths. Compared with the simulation results (using FEM with a gap $\delta = 0$ mm), the measured magnetization noise increases by 34.1%, and the simulated magnetization noise increases by 4.9%–29.3% with $\delta = 0.01$ mm–0.10 mm. The simulations also indicate that the average gap width of the real ferrite shield is close to 0.10 mm. This gap width ($\delta = 0.1$mm) is close to the estimated value in Section III. A ($\delta = 0.05$–0.1 mm). The difference may be attributed to the nonuniformity of the gap width and the inconsistency of the ferrite components, which were not considered in our analysis. If the gap width can be reduced to be smaller than 0.01 mm, the increase of the magnetization noise will be less than 4.9%, which can be negligible in practical applications.

IV. CONCLUSION

In this study, we developed a cylindrical ferrite shield that consisted of multiple ferrite annuli and lids. This structure can be fabricated and machined more easily compared the entire module, albeit at the cost of creating gaps between different parts. We measured the magnetic noise of the ferrite shield and used FEM to analyze the effects of the gaps. Our study indicated that compared with the ferrite shield without gaps, the magnetization noise increased by 34.1%. Nonetheless, the magnetization noise still achieved $5.5f^{-1/2}$ fT. This level of magnetic noise is analogous to the performance of ferrite shields without gaps, and considerably lower than that for a similar-sized μ-metal shield. If the gap width is reduced to be smaller than 0.01 mm, the increase of the magnetization noise would be less than 4.9%, which can be negligible in practical applications. Therefore, the mating surfaces should be polished as smooth as possible to reduce the gap width. The optimization of the dimensions of the multi-annular ferrite shield to further reduce the magnetic noise would be carried out in the future work.

REFERENCES

[1] C. Zhang, H. Yuan, Z. Tang, W. Quan, and J. C. Fang, "Inertial rotation measurement with atomic spins: From angular momentum conservation to quantum phase theory," *Appl. Phys. Rev.*, vol. 3, no. 4, Dec. 2016, Art. no. 041305.

[2] J. Kitching, "Chip-scale atomic devices," *Appl. Phys. Rev.*, vol. 5, no. 3, Sep. 2018, Art. no. 031302.

[3] W. Fan, W. Quan, W. Zhang, L. Xing, and G. Liu, "Analysis on the magnetic field response for nuclear spin co-magnetometer operated in spin-exchange relaxation-free regime," *IEEE Access*, vol. 7, pp. 28574–28580, 2019.

[4] E. A. Donley, E. Hodby, L. Hollberg, and J. Kitching, "Demonstration of high-performance compact magnetic shields for chip-scale atomic devices," *Rev. Sci. Instrum.*, vol. 78, no. 8, Aug. 2007, Art. no. 083102.

[5] T. G. Walker and M. S. Larsen, "Spin-exchange-pumped NMR gyros," *Adv. At., Mol., Opt. Phys.*, vol. 65, pp. 373–401, Jan. 2016.

[6] K. Nishi, Y. Ito, and T. Kobayashi, "High-sensitivity multi-channel probe beam detector towards MEG measurements of small animals with an optically pumped K-Rb hybrid magnetometer," *Opt. Express*, vol. 26, no. 2, pp. 1988–1996, Jan. 2018.

[7] F. Thiel, A. Schnabel, S. Knappe-Grneberg, D. Stollfu, and M. Burghoff, "Proposal of a demagnetization function," *IEEE Trans. Magn.*, vol. 43, no. 6, pp. 2959–2961, Jun. 2007.

[8] I. Altarev, M. Bales, D. H. Beck, T. Chupp, K. Fierlinger, P. Fierlinger, F. Kuchler, T. Lins, M. G. Marino, B. Niessen, G. Petzoldt, U. Schläpfer, A. Schnabel, J. T. Singh, R. Stoepler, S. Stuiber, M. Sturm, B. Taubenheim, and J. Voigt, "A large-scale magnetic shield with 10^6 damping at millihertz frequencies," *J. Appl. Phys.*, vol. 117, no. 18, May 2015, Art. no. 183903.

[9] I. K. Kominis, T. W. Kornack, J. C. Allred, and M. V. Romalis, "A subfemtotesla multichannel atomic magnetometer," *Nature*, vol. 422, no. 6932, pp. 596–599, Apr. 2003.

[10] T. W. Kornack, S. J. Smullin, S.-K. Lee, and M. V. Romalis, "A low-noise ferrite magnetic shield," *Appl. Phys. Lett.*, vol. 90, no. 22, May 2007, Art. no. 223501.

[11] S.-K. Lee and M. V. Romalis, "Calculation of magnetic field noise from high-permeability magnetic shields and conducting objects with simple geometry," *J. Appl. Phys.*, vol. 103, no. 8, Apr. 2008, Art. no. 084904.

[12] J. Nenonen, J. Montonen, and T. Katila, "Thermal noise in biomagnetic measurements," *Rev. Sci. Instrum.*, vol. 67, no. 6, pp. 2397–2405, Jun. 1996.

[13] H. B. Dang, A. C. Maloof, and M. V. Romalis, "Ultrahigh sensitivity magnetic field and magnetization measurements with an atomic magnetometer," *Appl. Phys. Lett.*, vol. 97, no. 15, Oct. 2010, Art. no. 151110.

[14] D. Budker and D. F. J. Kimball, *Optical Magnetometry*. Cambridge, MA, USA: Cambridge Univ. Press, 2013, pp. 238–240.

[15] C. T. Munger, Jr., "Magnetic Johnson noise constraints on electron electric dipole moment experiments," *Phys. Rev. A, Gen. Phys.*, vol. 72, no. 1, 2005, Art. no. 012506.

[16] R. Mhaskar, S. Knappe, and J. Kitching, "A low-power, high-sensitivity micromachined optical magnetometer," *Appl. Phys. Lett.*, vol. 101, no. 24, Dec. 2012, Art. no. 241105.

[17] I. Savukov, Y. J. Kim, V. Shah, and M. G. Boshier, "High-sensitivity operation of single-beam optically pumped magnetometer in a kHz frequency range," *Meas. Sci. Technol.*, vol. 28, no. 3, Feb. 2017, Art. no. 035104.

[18] M. Smiciklas, J. M. Brown, L. W. Cheuk, S. J. Smullin, and M. V. Romalis, "New test of local lorentz invariance using a ^{21}Ne-Rb-K comagnetometer," *Phys. Rev. Lett.*, vol. 107, no. 17, 2011, Art. no. 171604.

[19] D. Bevan, M. Bulatowicz, P. Clark, J. Flicker, R. Griffith, M. Larsen, M. Luengo-Kovac, J. Pavell, A. Rothballer, D. Sakaida, E. Burke, J. Campero, B. Ehrsam, S. Estrella, and G. Morrison, "Nuclear magnetic resonance gyroscope: Developing a primary rotation sensor," in *Proc. IEEE Int. Symp. Inertial Sensors Syst. (INERTIAL)*, Moltrasio, Italy, Mar. 2018, pp. 1–2.

[20] M. C. D. Tayler, T. Theis, T. F. Sjolander, J. W. Blanchard, A. Kentner, S. Pustelny, A. Pines, and D. Budker, "Invited review article: Instrumentation for nuclear magnetic resonance in zero and ultralow magnetic field," *Rev. Sci. Instrum.*, vol. 88, no. 9, Sep. 2017, Art. no. 091101.
[21] *Large Size Ferrite Cores for High Power T/UU/UI/EC/EIC/EE/EI/DT/PQ/SP Series*, TDK, Tokyo, Japan, 2013.
[22] *Solutions for Measuring Permittivity and Permeability With LCR Meters and Impedance Analyzers—Application Note*, Santa Rosa, CA, USA, Keysight, 2017.
[23] *Cores Made of Soft Magnetic Materials Measuring Methods Part 2: Magnetic Properties at Low Excitation Level*, document IEC 62044-2, 2005.
[24] K. Yang, J. Lu, M. Ding, J. Zhao, D. Ma, Y. Li, B. Xing, B. Han, and J. Fang, "Improved measurement of the low-frequency complex permeability of ferrite annulus for low-noise magnetic shielding," *IEEE Access*, vol. 7, pp. 126059–126065, 2019.
[25] R. M. Bozorth, *Ferromagnetism*. New York, NJ, USA: IEEE Press, 1993, p. 476.
[26] Y. Singh, "Electrical resistivity measurements: A review," *Int. J. Mod. Phys., Conf. Ser.*, vol. 22, pp. 745–756, Jan. 2013.
[27] J. L. Kirschvink, "Uniform magnetic fields and double-wrapped coil systems: Improved techniques for the design of bioelectromagnetic experiments," *Bioelectromagnetics*, vol. 13, no. 5, pp. 401–411, 1992.
[28] S. Jeon, G. Jang, H. Choi, and S. Park, "Magnetic navigation system with gradient and uniform saddle coils for the wireless manipulation of microrobots in human blood vessels," *IEEE Trans. Magn.*, vol. 46, no. 6, pp. 1943–1946, Jun. 2010.
[29] J. Lu, W. Quan, M. Ding, L. Qi, and J. Fang, "Suppression of light shift for high-density alkali-metal atomic magnetometer," *IEEE Sensors J.*, vol. 19, no. 2, pp. 492–496, Jan. 2019.
[30] D. Ma, M. Ding, J. Lu, H. Yao, J. Zhao, K. Yang, J. Cai, and B. Han, "Study of shielding ratio of cylindrical ferrite enclosure with gaps and holes," *IEEE Sensors J.*, vol. 19, no. 15, pp. 6085–6092, Aug. 2019.
[31] Z. Kubík and J. Skála, "Shielding effectiveness simulation of small perforated shielding enclosures using FEM," *Energies*, vol. 9, no. 3, p. 129, Feb. 2016.

JIXI LU received the Ph.D. degree in measurement technology and instruments from Beihang University, Beijing, China, in 2016. He is currently an Assistant Professor with the Research Institute for Frontier Science, Beihang University. His research interests include atomic magnetometers and magnetic shield.

DANYUE MA received the B.E. degree in mechanical engineering and automation from the Beijing University of Technology, Beijing, China, in 2016. She is currently pursuing the Ph.D. degree with Beihang University, Beijing. Her current research interest is in magnetic shield.

KE YANG received the B.E. degree in information engineering from Beihang University, Beijing, China, in 2016, where he is currently pursuing the Ph.D. degree. His current research interest is in atomic magnetometer.

WEI QUAN received the Ph.D. degree in precision instrument and mechanics from Beihang University, Beijing, China, in 2008. He is currently a Professor with the Research Institute for Frontier Science, Beihang University. His current research interests include atomic spin inertial measurement, atomic magnetometers, and information fusion navigation.

JUNPENG ZHAO received the B.E. degree in measurement and control technology and instrumentation from the Hebei University of Technology, Tianjin, China, in 2015. He is currently pursuing the Ph.D. degree with Beihang University, Beijing, China. His research interest is in atomic polarization.

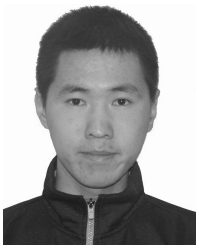

BOZHENG XING received the B.E. degree in information engineering from Beihang University, Beijing, China, in 2017, where he is currently pursuing the Ph.D. degree. His current research interests include atomic magnetometers and optical detection.

BANGCHENG HAN received the Ph.D. degree in mechanical manufacture and automation from the Changchun Institute of Optics, Fine Mechanics and Physics, Chinese Academy of Sciences, Changchun, China, in 2004. He is currently a Professor with the School of Instrumentation and Optoelectronic Engineering, Beihang University, Beijing, China. His research interests include mechatronics, magnetic suspension technology, attitude control actuator of spacecraft, and precision measurement.

MING DING received the Ph.D. degree in optoelectronics from the Optoelectronics Research Centre, Optical Fiber Nanowires and Related Devices Group, University of Southampton, Southampton, U.K., in 2013. She is currently a Professor with the Research Institute for Frontier Science, Beihang University, Beijing, China. Her current research interests include atomic magnetometer, microresonator and nanoresonator, and microfiber and nanofiber.